Local strains in a beam and slab bridge model under concentrated load

Local Strains in a Beam and Slab Bridge Model Under Concentrated Load

Sollicitations locales au modèle d'un pont en poutres et plaques sous charge concentrée

Örtliche Beanspruchungen am Modell einer Balken- und Plattenbrücke unter konzentrierter Belastung

YEW-CHAYE LOO
Ph. D., Research Fellow, University of Dundee
Great Britain

Introduction

General Remarks

In the analysis of local plate bending moments in the top slabs of spine box girder bridges or in the slabs of beam and slab decks, the equations given by WESTERGAARD [1] are still widely used. The equations for slab moment due to concentrated load acting at a position between webs were derived by Westergaard for an infinitely long strip with either simply-supported or fixed edges. In other words, effects due to the rigidities of the webs or beams are not considered in the Westergaard analysis. Attempts have also been made recently by SAWKO and MILLS [2] to find a simple approach for the design of cantilever slabs for spine box bridge decks. The same fixed edge assumption is used in their approach and as with the Westergaard analysis no provision has been given for the determination of longitudinal plate moments.

Due to the general availability of high speed computers, sophisticated methods have been developed for the analysis of folded plate type structures which includes the type of bridge deck mentioned above. Folded plate theory, the finite element method and the finite strip approach are three comparatively well-known techniques available. Thin plate theories for bending and in-plane stress analysis are normally adopted in these computer-based methods. Harmonic functions are incorporated in the elasticity theory of folded plate analysis; polynomial functions are used in a finite element procedure on the discretized model; a combination of harmonic functions and polynomials is adopted in the finite strip approach. Although various features of different forms of bridge construction can be effectively included, the accuracy of these analyses depends greatly on the number of harmonics used or the fineness of the discretization adopted or a combination of both variations in the solution. It is a well-known fact that at points where concentrated load acts, thin plate theory would give infinite values for bending moments in the transverse and longitudinal directions. Previous experiments carried out by CUSENS and PAMA [3] and LIM and MOFFATT [4] show that in slab-type bridge decks, bending moment profiles with very high peaks are actually produced by concentrated loads. This immediately poses a question as to the number of harmonics or to the fineness of the discretization to be used to obtain satisfactory bending moments under concentrated load for folded-plate structures. Unfortunately, most of the previous workers [5], [6] in this field end their research more or less with the successful development of computer programs. Undoubtedly, in view of the thin plate assumptions used in developing these programs, over-conservative solutions can always be obtained by adopting a very fine discretization and/or a great number of harmonics. However, in practice, an over-estimate in a solution is as undesirable as inadequate analysis. It is therefore clear that if the various solutions for folded plate structures are to be used effectively in predicting local bending moments in box and T-beam bridge decks, experimental data are needed to set up practical convergence criteria for the respective computer-based analyses.

The Finite Strip Programs

As part of the research programme sponsored by the Construction Industry Research and Information Association on bridge deck structures carried out in the University of Dundee, two computer programs based in the finite strip procedure have been developed by the author in collaboration with CUSENS [7]. The first program is based on the conventional finite strip approach for folded plate structures with simple end support conditions. The procedure was originated by CHEUNG [5], [8] using a "third order" bending displacement function in conjunction with a "linear" function representing the in-plane displacement field. The second program of LOO and CUSENS incorporates the auxiliary nodal line (ANL) technique [9] for the analysis of simply-supported box-girder bridge decks by the finite strip method. Fifth order bending and second order in-plane displacement functions are used to develop the property matrices for a strip with one auxiliary nodal line at the mid-width of the strip. The conventional strip and the strip with one ANL may be seen in Fig. 1. Since the unknown deformation amplitudes associated with the auxiliary nodal lines can be eliminated before the assembling procedure which leads to

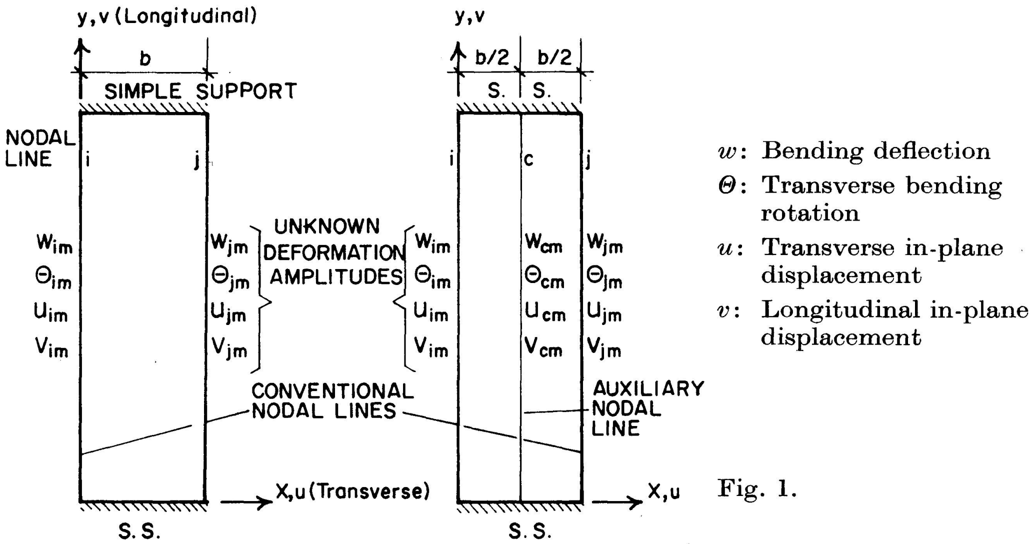

Fig. 1.

the overall stiffness matrix, the resulting band width for a particular strip simulation is identical to that of the conventional approach. This means that, for the ANL procedure, the solution time in a computer will only be marginally higher than the lower order approach. However, the ability of the higher order strip in simulating the actual displacement and stress fields is considerably increased.

Object and Scope of Study

In order to gain a better understanding of the convergence behaviour of the two finite strip programs and thus to guide users of the programs in the evaluation of local plate bending moments, an approximately $^1/_{30}$ scale asbestos-cement T-beam bridge model was built and tested under concentrated loads. Since the model was made up of a top slab and only two longitudinal deep beams, it could be regarded as a single-cell spine-box bridge without a bottom slab. As far as local plate bending characteristics are concerned, the model reflects the behaviour of a true spine-box bridge deck.

The distribution of local strains under concentrated load at various load positions has been thoroughly investigated using electrical resistance strain gauges. Results are compared with the computer analyses based on the two finite strip programs. Five mm and ten mm crossed-gauges and rosettes were used. The strains measured by the two sizes of gauges under similar loading conditions are compared with each other. In the light of the experimental data a study was made of the convergence characteristics of the two above-mentioned finite strip programs in predicting local plate strains in the top slab of the model under concentrated loads. As a result, criteria may be set up for the two programs to yield satisfactory results of local bending moments in folded plate type bridge decks under wheel loadings. Such criteria include the required discretization pattern and the appropriate harmonic numbers retained for the solutions.

This paper deals mainly with the behaviour of the bridge model and with some comparisons of results. In addition, the effect of patch loads and the distribution of in-plane strains at longitudinal beams are also studied. Finally comparison is made between the finite strip (ANL) procedure and the Westergaard approach in predicting local plate bending moments.

Description of the Asbestos Cement Beam and Slab Bridge Model

The asbestos cement beam and slab bridge model was fabricated by joining together the component parts to form the required structure. Two $\frac{1}{2}$-in. thick longitudinal strips were first glued to two 1-in. thick end diaphragms using CIBA Aerodux 500.F with Hardener 501. Then a $\frac{3}{8}$-in. slab was connected to the grid using the same mixture of adhesive to form the T-beam model. In every connection, a pressure of about 1.5 lbf/sq-in was applied to the joints for 18 hours. Since the adhesive has gap-filling properties, higher pressure is not necessary to give firm contact. The first test was conducted ten days after the model was completed. Preliminary investigations showed that such connections resembled rigid joints up to a flexure stress of 1500 lbf/in^2 where a sudden failure might occur. In view of this finding maximum stress at joints between slab and beams were kept well below the limit. A detailed drawing of the model is shown in Fig. 2.

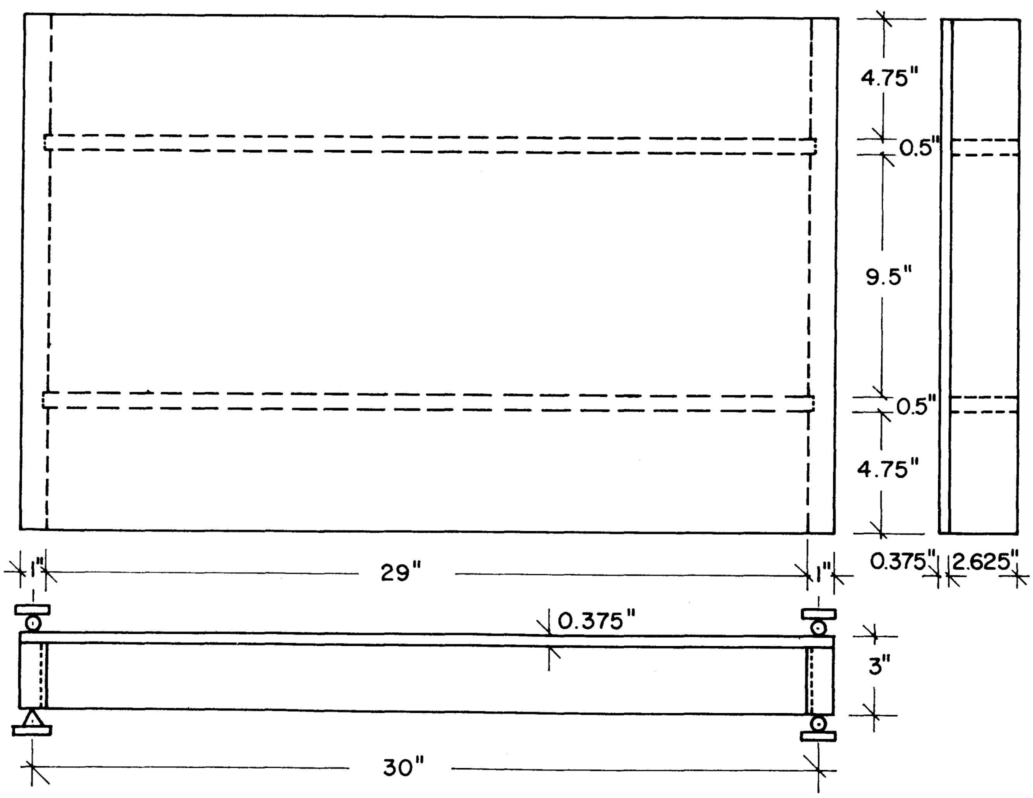

Fig. 2.

For the $\frac{3}{8}$-in. thick top slab, four control specimens (two in each orthogonal direction) were cut from the same sheet of material. Two $\frac{1}{2}$-in. thick specimens (one in each direction) were prepared from the same sheet as the two longitudinal beams. In obtaining the values of modulus of elasticity and Poisson's ratio for the different specimens the simple beam method was used. The dimensions, test set-up and the corresponding elastic constants for the different specimens are given in Table 1.

Table 1. Details of Control Specimens

Specimen Number	Dimensions $b \times l \times t$ (in³)	E.R.S.G.*) Used	Test Set-Up	E_x**)	E_y**)	ν
1	$1 \times 11.5 \times \frac{3}{8}$	10 C 5 R 10 C	3.5″ ↓ 4.5″ ↓ 3.5″	2.64 2.51 2.83		0.185 0.192 0.190
2	$1 \times 11.5 \times \frac{3}{8}$	10 C 5 R 10 C	3.5″ ↓ 4.5″ ↓ 3.5″		2.76 2.83 2.91	0.188 0.186 0.184
3	$2 \times 15 \times \frac{3}{8}$	5 R 5 C 5 R 10 C	5″ ↓ 5″ ↓ 5″	2.79 2.81 2.90 2.98		0.185 0.176 0.189 0.185
4	$2 \times 15 \times \frac{3}{8}$	5 R 10 C 5 C 5 R	5″ ↓ 5″ ↓ 5″		2.86 3.09 3.43 2.67	0.199 0.200 0.180 0.184
Average (Top Slab)				2.78	2.94	0.187
5	$1 \times 9.5 \times \frac{1}{2}$	10 C 10 C 5 C	5.5″ ↓ 4″	3.44 3.96 3.85		0.194 0.188 0.184
6	$1 \times 15 \times \frac{1}{2}$	10 C 10 C 5 R	5″ ↓ 5″ ↓ 5″		3.63 3.86 4.16	0.200 0.191 0.243
Average (Beams)				3.75	3.88	0.200

*) 5 C = 5 mm Crossed gauge
5 R = 5 mm Rosette
10 C = 10 mm Crossed gauge

**) $\times 10^6$ lbf/in²

The model was supported in a steel rig on a knife edge at one end and a $\frac{1}{4}$-in. diameter roller on the other. Possible uplift was prevented by two $\frac{1}{4}$-in. rollers at the ends as shown in Fig. 2. Loading was applied using a simple lever system and the concentrated load was applied through a $\frac{1}{2}$-in. diameter steel bearing. In the patch loading tests, $\frac{1}{2}$-in. thick square asbestos cement pads were used to transmit load. To ensure even contacts, electrical insulating tape was placed between the patch load and the loaded surface of the top slab. A general view of the test set-up is given in Fig. 3.

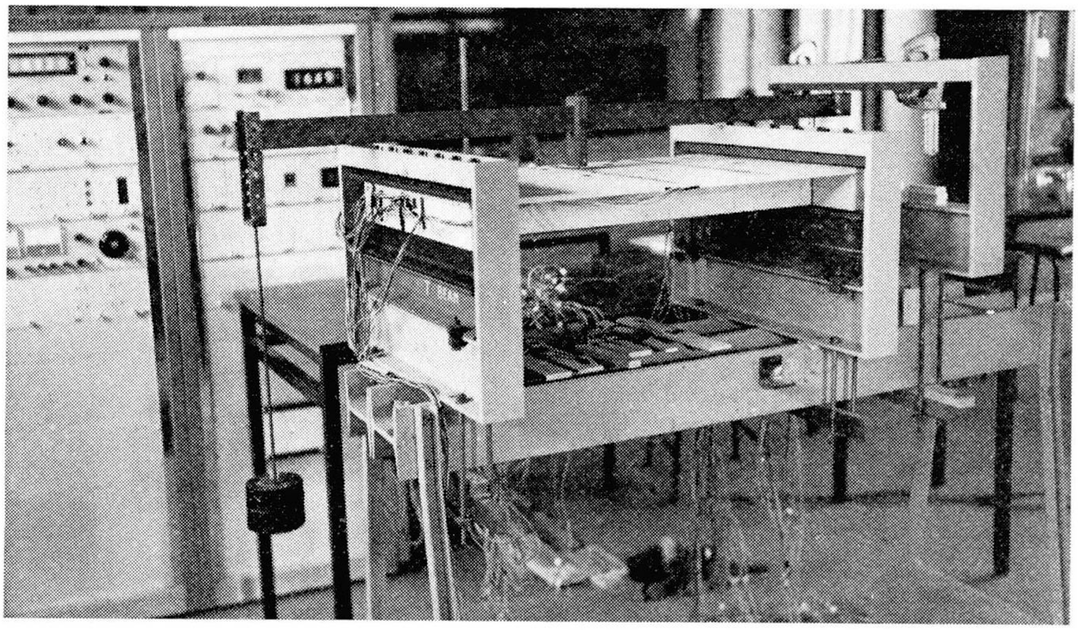

Fig. 3. Model test set-up and the data logger.

Instrumentation and Test Procedure

The primary aim of this experiment was to study the distribution of local plate bending moments due to concentrated loads so that it was necessary to measure the magnitude of strains at points immediately under the load. In order to deduce in-plane stresses and bending moments at a point in a folded-plate structure both top and bottom surface strain measurements were required. For obvious reasons it is difficult to measure the top surface strain at points where the load is actually applied and electrical resistance gauges were fixed only at the bottom surface of the top slab. Comparisons with theoretical results were possible only for the bottom fibres of the slab. However, since the model was so designed that the in-plane stresses under the load contributed in most cases a very small percentage of the total strain, a good reflection of the distribution characteristics for local bending moments was achieved.

Preliminary investigations using the finite strip programs showed that local bending moment profiles with very pronounced peaks could be induced by a concentrated load on the model. Theoretically, strain gauges of the smallest possible size should be used to pick up these high concentrated strains. The larger the gauge length, the lower is the strain which would be recorded. However, in view of the difficulty of proper alignment for the gauges (at the bottom surface) with the applied loads (at the top surface), very small electrical resistance gauges have not been adopted. Instead, 5 mm crossed-gauges and rosettes (45-degree) and 10 mm crossed-gauges were used at the top slab of the model to detect possible differences in measured strains under the same

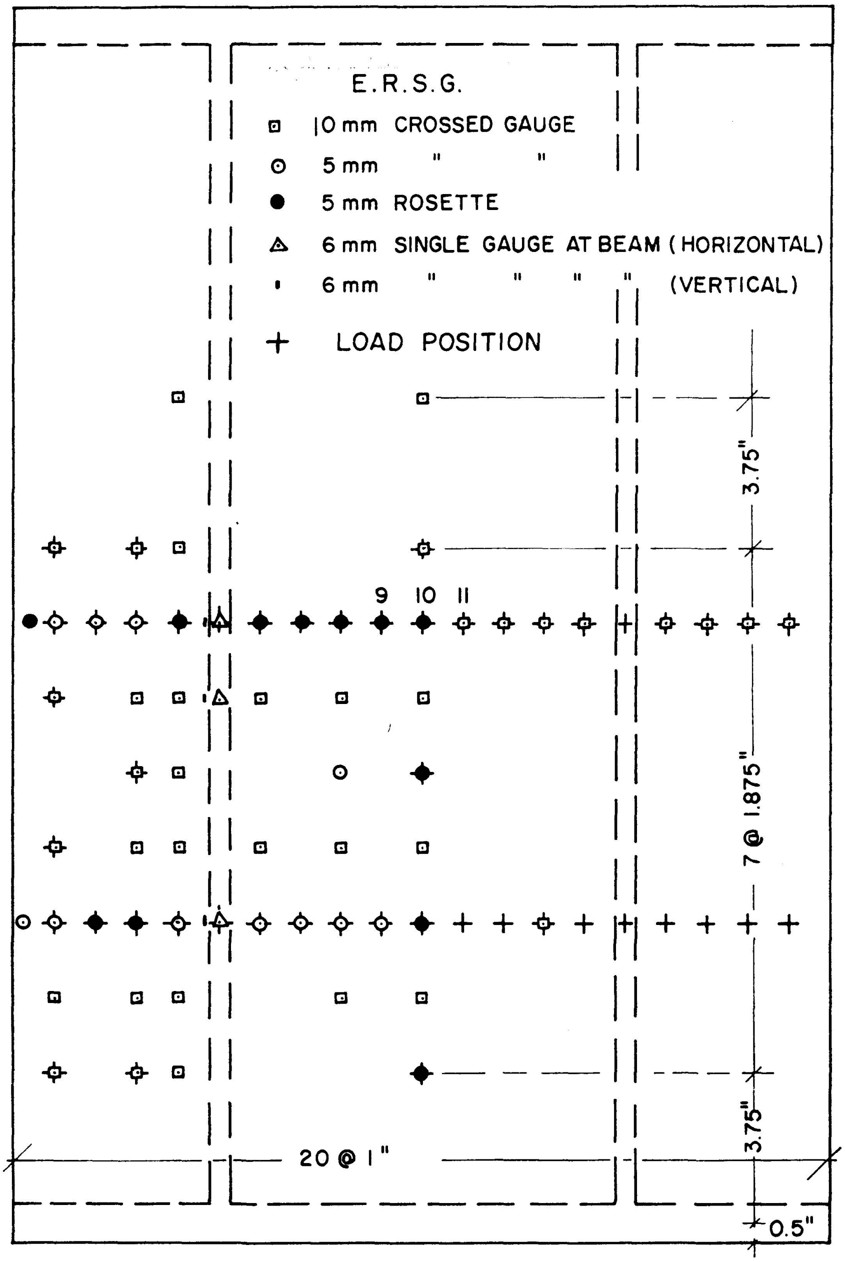

Fig. 4.

loading condition. Six mm single gauges were also fixed to the longitudinal beams of the model. For each crossed-gauge or rosette it is possible to measure accurately the transverse and longitudinal strains at a common point. The layout of gauge positions at the model is given in Fig. 4 together with the loading positions. It can be seen from Fig. 4 that at the mid-span of the bridge, 5 mm and 10 mm gauges were attached respectively to the two symmetrical halves of the mid-span line. This arrangement was to provide a check on possible differences in recorded strains by the two sizes of gauges. The effective width and length of the 5 mm gauge are 1.6 mm and 5 mm respectively; if scaled to the prototype dimensions this represents an area of approximately 2×6 in^2. Similarly, the effective dimensions of the 10 mm gauge are equivalent to an area of 4×12 in^2 in a prototype structure. These gauges were connected to a data logger as may be seen in Fig. 3.

For every loading position, four increments of load in the range of 30, 40, 50 and 60 lbf were applied to the model. The strain gauges were scanned by the data logger and the voltage readings for all gauges were punched out on paper tape at the rate of one gauge per second. The punched tape was fed directly to the computer and a program was written to convert the voltage readings into strains. For each resistance gauge, the strains corresponding to the four load increments were printed out together with the mean value. These mean strains are used in the comparisons with the computer analyses. The model and the strain gauges behaved well and linear behaviour was noted throughout the experiments. Fig. 5 shows some typical load-strain curves for the model tests.

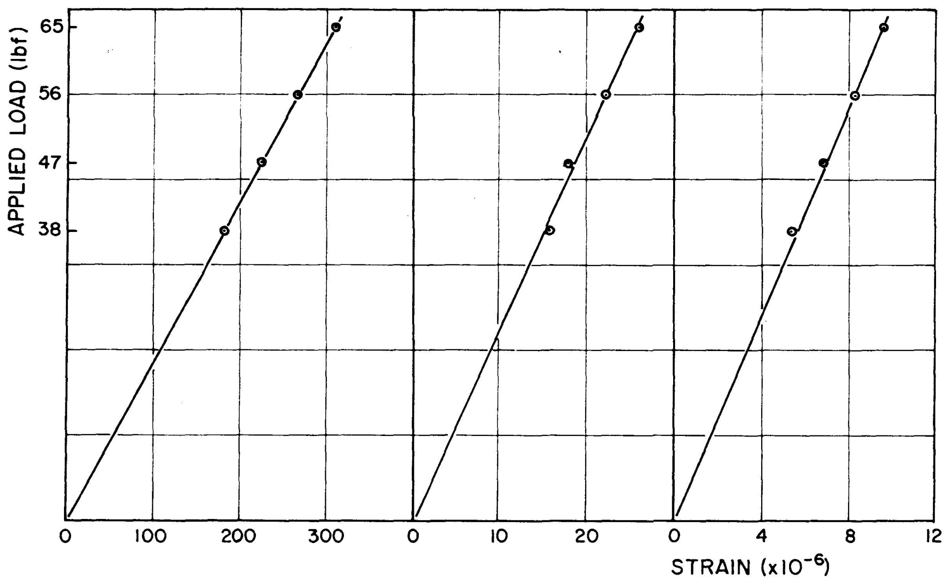

Fig. 5.

After the major concentrated load tests were completed, square patch loads with patch areas of 1, 0.5625, 0.25 and 0.0625 in^2 respectively were applied at load positions 9, 10 and 11 (see Fig. 4). Similar loading increments were used but only the strain readings for gauges at the mid-span were recorded.

Finite Strip Analyses of the Model

The model was analysed using the two finite strip programs developed for the analysis of box girder bridge decks with simple end supports. All the experimental load positions have been considered. In fact, in order to plot some of the theoretical curves more completely, additional load positions near the support were analysed. Concentrated force matrices were used to represent the applied loads. For convenience, and to conform with the loading positions across the width of the model, 20 strips (each of 1-in. width) were used to simulate the top slab and a total of 6 strips (each of 0.9385-in. width) were used for the two longitudinal beams. The real and simulated structures are shown in Fig. 6. The elastic constants used are the means of the values given by the control specimen tests (see Table 1).

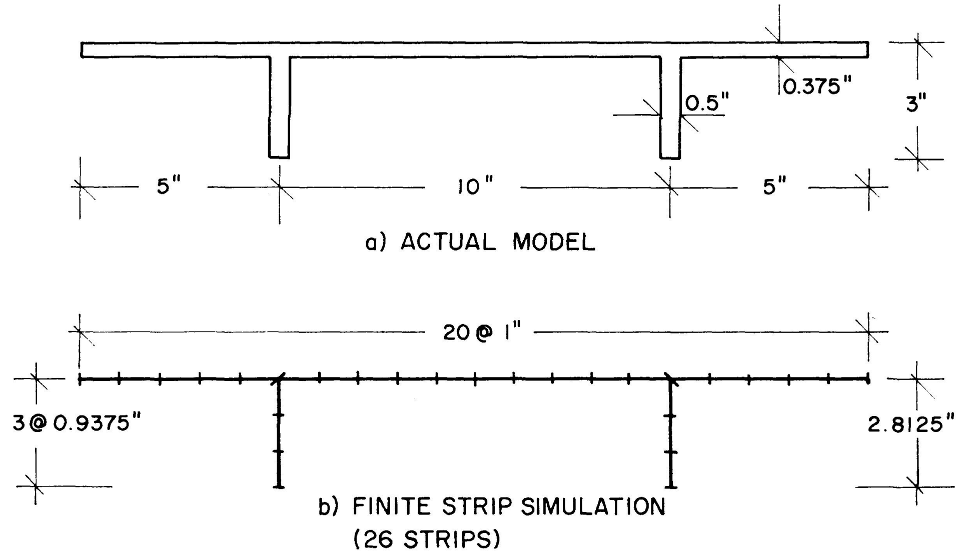

Fig. 6.

In all of the comparisons given in the following sections, the theoretical values are the algebraic sums of the in-plane and bending strains. The average values given by the two adjacent strips at the nodal line were used throughout.

Convergence Curves of the Finite Strip Procedures for Local Bending Strains

In order to study the comparative convergence characteristics of the conventional finite strip procedure and the higher order strip approach (with one auxiliary nodal line), theoretical strain values were plotted against the number of harmonics. Experimental strains are also included in these "convergence" curves so that a clear comparison between analytical and experimental results can be obtained. Convergence curves for all the experimental load positions have been drawn but only two positions at mid-span are presented in Fig. 7. It can be seen in Fig. 7 that the ANL procedure is superior to the conventional program in giving transverse strain values. A marginally better convergence is given by the higher order analysis in longitudinal strains. This big improvement in the transverse strain evaluation is no doubt due to the more flexible polynomial functions used for the transverse direction in the finite strip formulation.

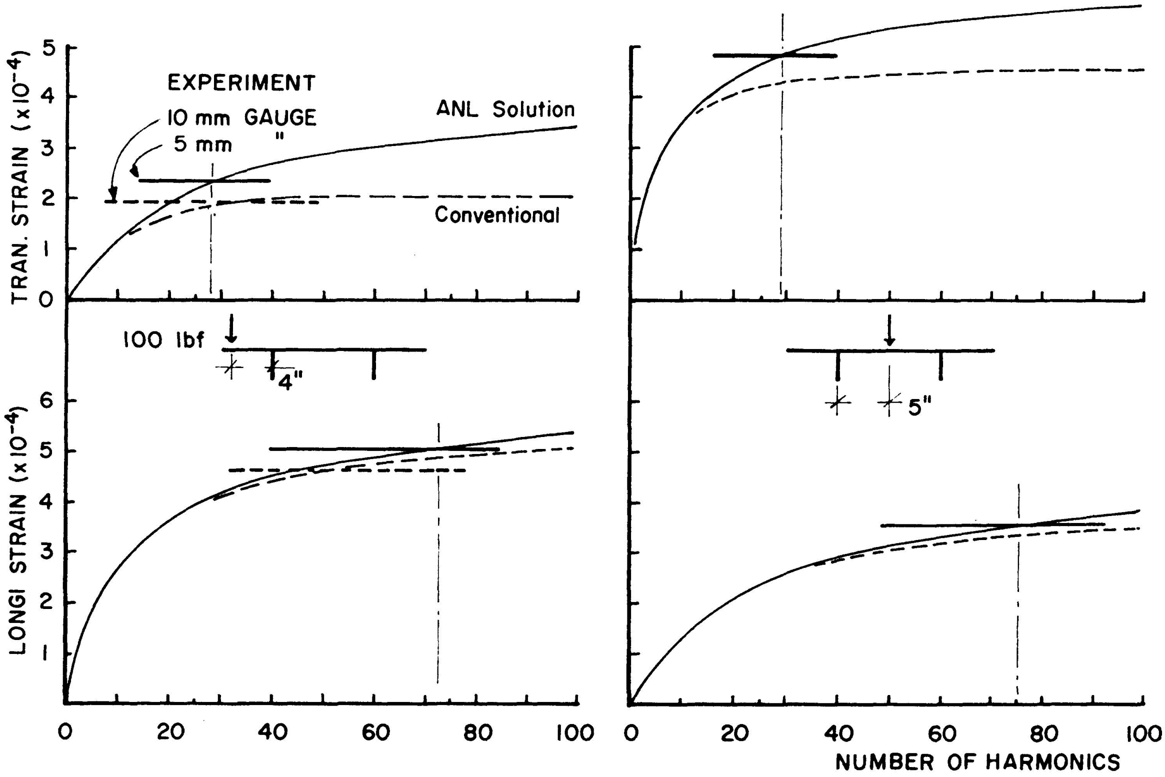

Fig. 7.

By a general survey of the convergence curves for various load positions including others not given here, it was found that the ANL solution requires 25 harmonics to give a satisfactory prediction of transverse strains as measured by the 5 mm gauges. On the other hand, the conventional procedure needs 45 harmonics to give close values of transverse strains using this particular strip idealization (see Fig. 6). For longitudinal strain values as recorded by the 5 mm gauges, a satisfactory evaluation will be given by the higher order program with 75 harmonics whereas the conventional solution requires 95 harmonics for a good correlation. This low rate of convergence for both programs for longitudinal bending strains may be attributed to the fact that in a Fourier series simulation for a discontinuous curve, it generally requires a great number of harmonics before a satisfactory shape can be achieved.

Variation of Maximum Strains Under a Moving Concentrated Load

In order to give an overall view of the variation of maximum local bending moments at top slab of the T-beam model, the strains under concentrated load have been plotted for various sections of the bridge. The transverse variations of maximum strains under a 100 lbf concentrated load, moving across the width of the model at mid-span and quarter span are given in

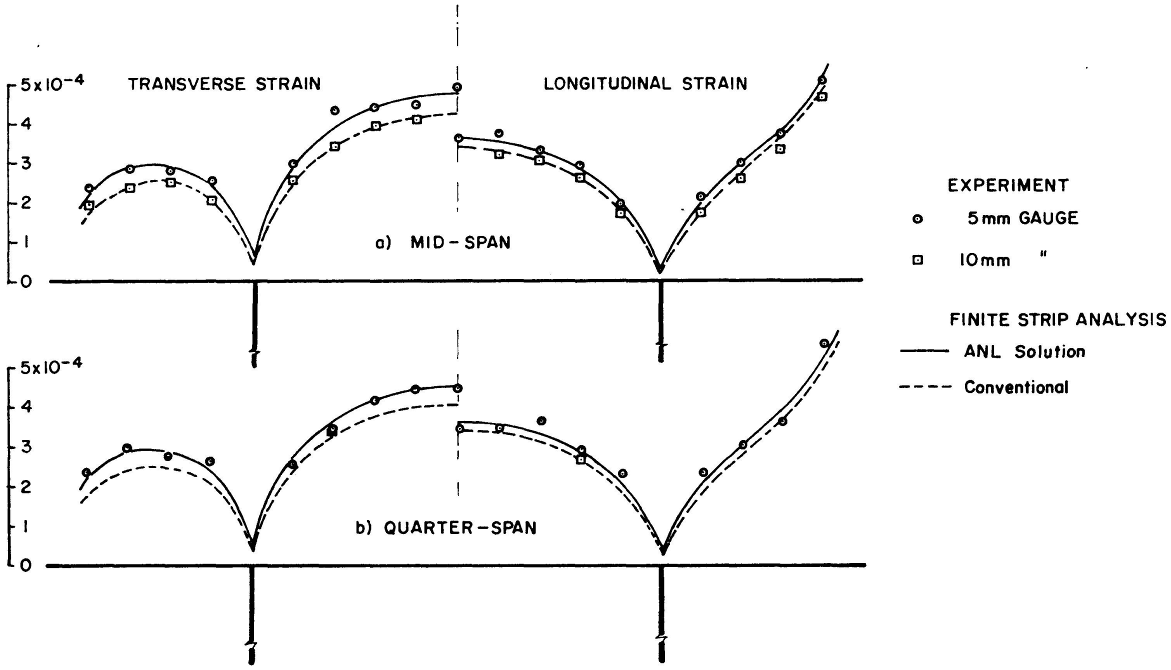

Fig. 8.

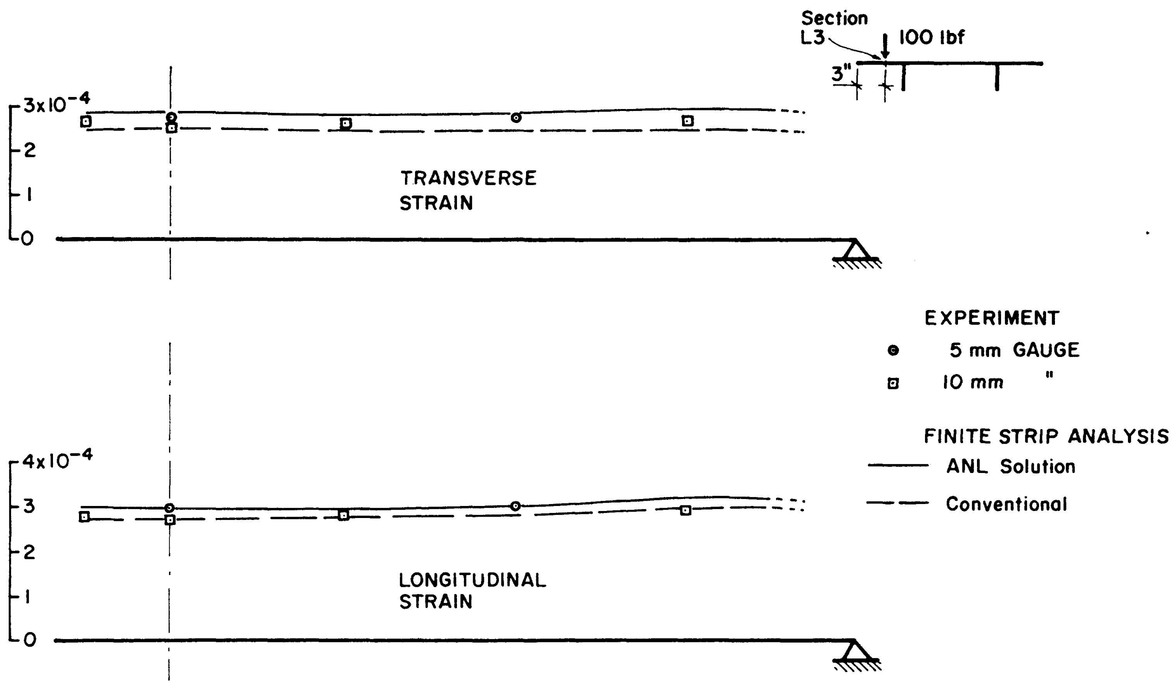

Fig. 9.

Figs. 8a and 8b respectively. Figs. 9 and 10 show respectively the variation of strains under the load at two different longitudinal sections. In these figures, experimental strains given by the 5 mm and 10 mm gauges are plotted together with the analytical results due to the two finite strip programs. In all these

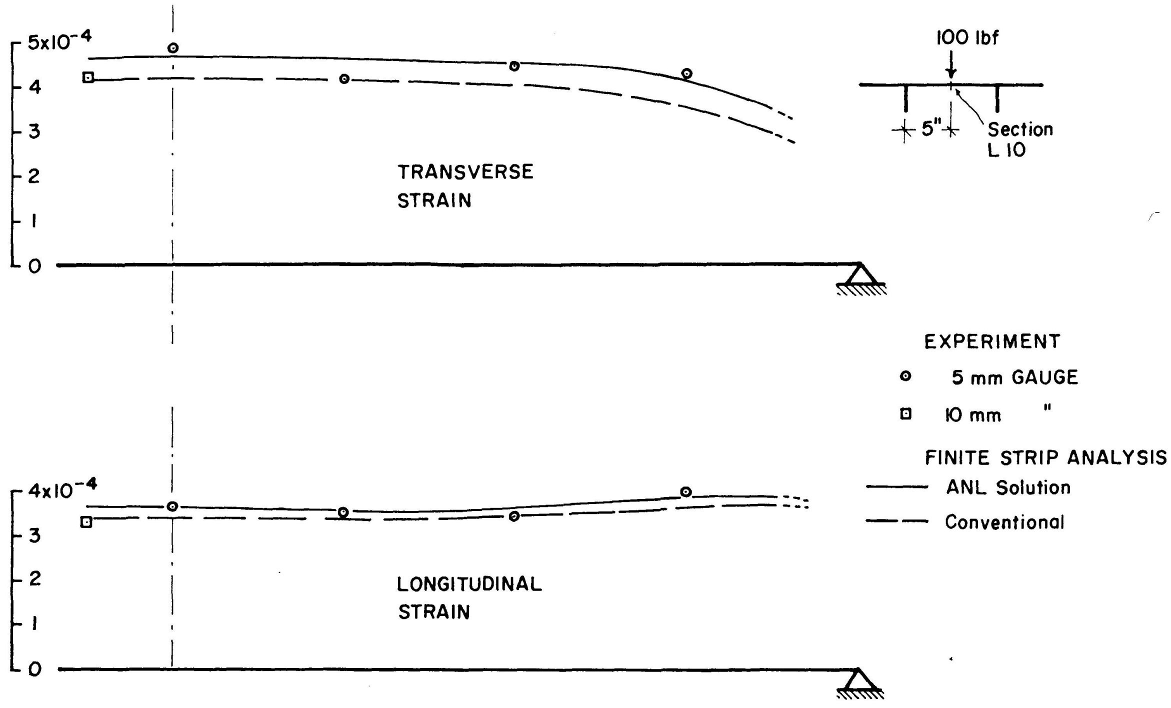

Fig. 10.

and subsequent comparisons, 25 and 75 harmonics are used respectively for the transverse and longitudinal strains given by the two computer programs. It is clear from Fig. 8a that for a same loading condition, the maximum strains under load given by the 10 mm gauges are consistently lower than those measured using 5 mm gauges. The reason for this is obvious since for this strain condition the smaller gauge covers a smaller strain field surrounding the peak which in turn gives a higher strain measurement.

The higher order analysis yields higher values of strains for the same strip idealization and an identical number of harmonics. It is interesting to see from Fig. 8a that the conventional analysis, though it underestimates the profiles given by 5 mm gauges, gives a very good correlation with those measured using 10 mm gauges.

An important phenomenon is revealed in Figs. 9 and 10. It may be seen in these graphs that the maximum transverse and longitudinal strains under the moving concentrated load as given by experiments and analyses are more or less constant throughout a large length of the span of the bridge. No obvious decrease in magnitudes for the measured strains at various sections can be seen even at points as close as 3.75 in. ($\frac{1}{8}$ span) from the diaphragm support (see Fig. 2). Analytical plots show that gradual drop for transverse strains commences only at points near the $^{1}/_{16}$-span line. This finding is useful from the designer's point of view. It provides sufficient justification to design the top slab of a box or T-beam bridge for local bending moments based on the analysis of only one section somewhere along the span of the bridge.

Transverse Distribution of Strains

The transverse distributions of transverse strains under load for selected load positions at mid-span and quarter-span are shown in Fig. 11. Fig. 12 gives the transverse distributions of longitudinal strains under concentrated load at the corresponding load positions. The experimental data are plotted with the ANL solution and with results by the conventional strip procedure given at selected profiles. It should be noted that, in obtaining all but one of the experimental points in the right half of the model at quarter span, symmetrical conditions have been assumed. It may be observed in Figs. 11 to 12 that excellent correlations with the experiments are given by the analysis based on finite strip with one auxiliary nodal line. The analysis by the conventional program gives good results at points remote from the applied load but underestimates the peak strains. It should be noted from Figs. 11b and 12b that for the symmetrical load the recorded strains by the 5 mm and 10 mm

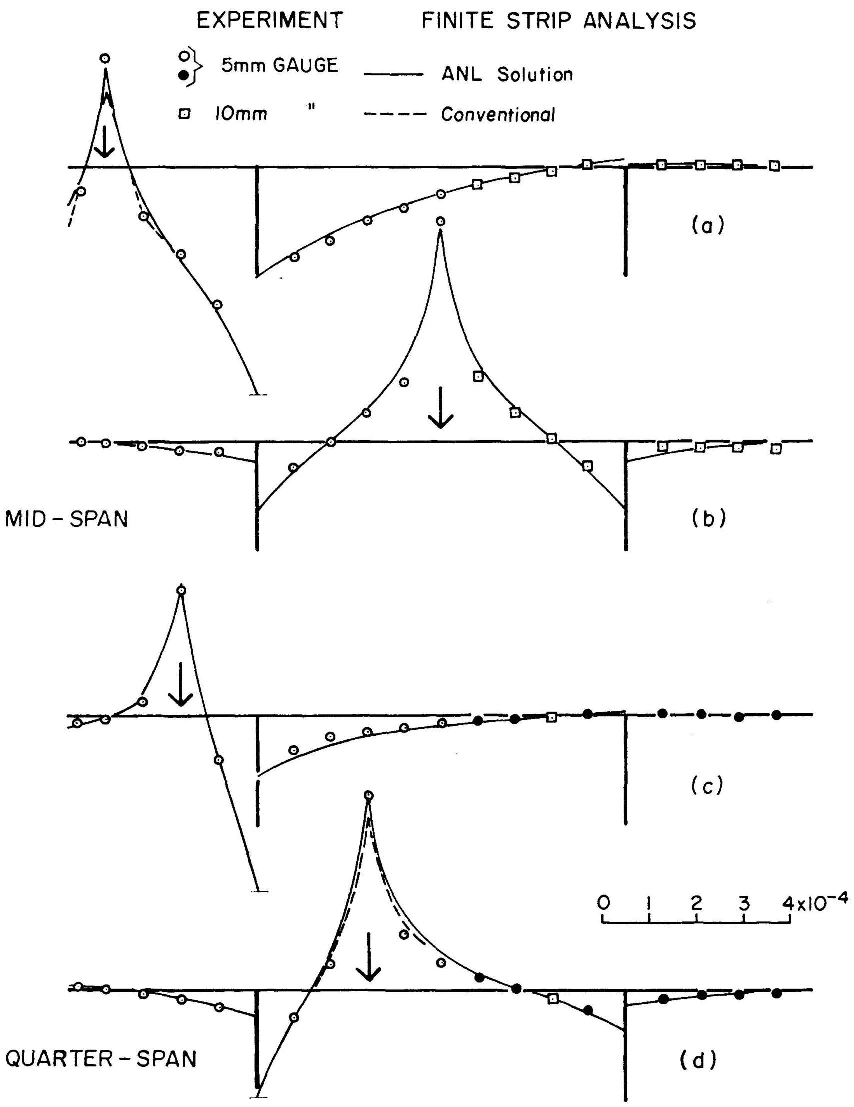

Fig. 11.

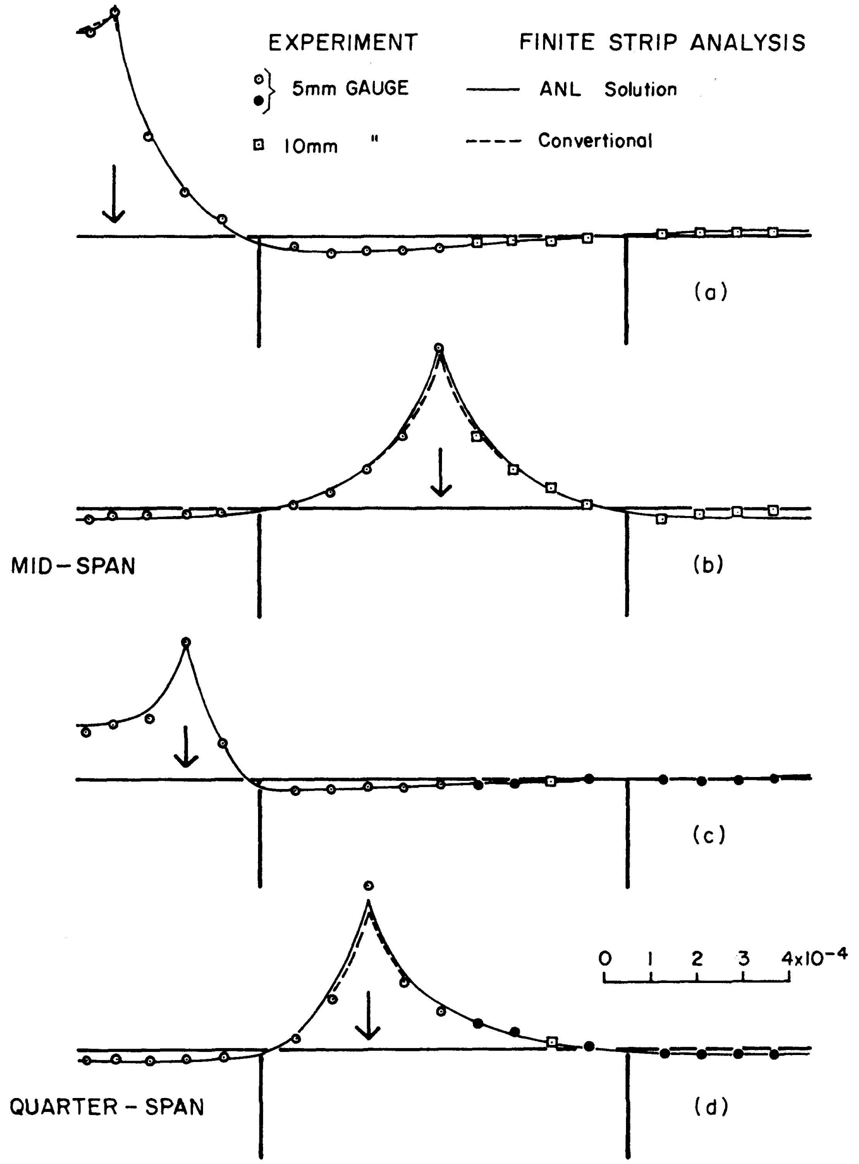

Fig. 12.

gauges are very close to each other at the corresponding symmetrical points. This is as expected since at positions far from the concentrated load the strain variation is more gentle; hence, the two types of gauges should yield similar values of strain.

Longitudinal Distribution of Strains

The distribution of transverse and longitudinal strains for two longitudinal sections due to concentrated load at different load positions is given in Figs. 13 to 17. It can be seen in these figures that the ANL analysis gives a close prediction of strains in both directions and, again for this particular simulation (see Fig. 6). On the other hand, the low order analysis underestimates the maximum strains under the loads but overestimates the transverse strains in regions next to the loads. This is mainly due to the fact that the third order

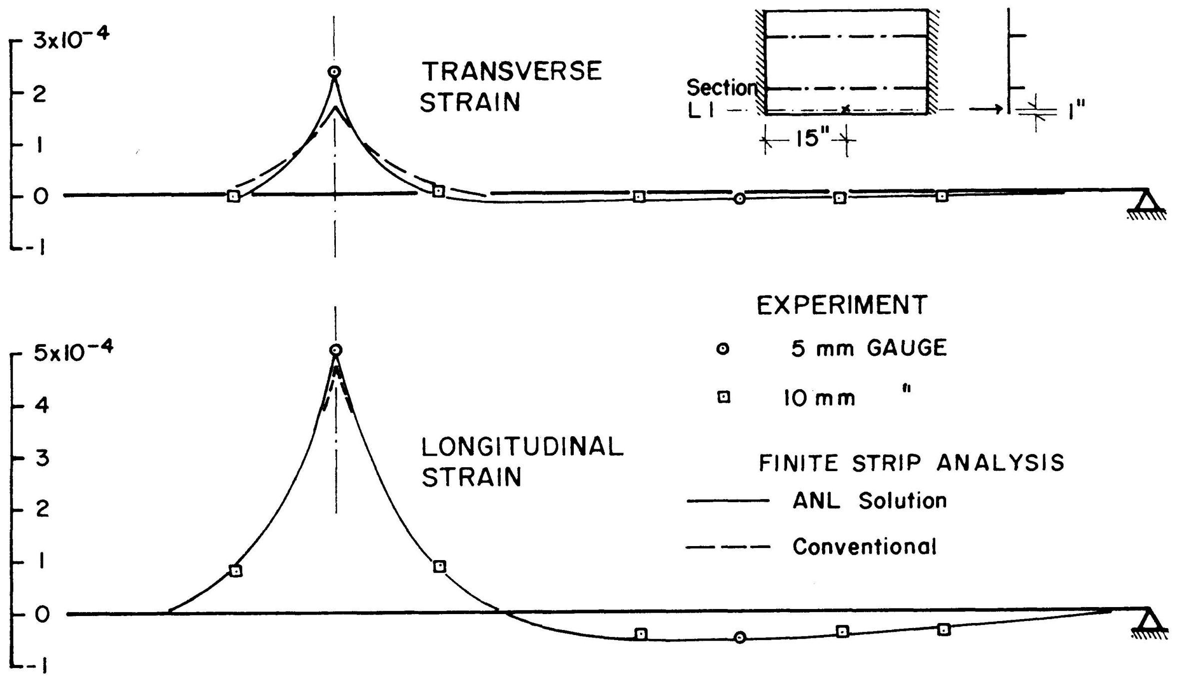

Fig. 13.

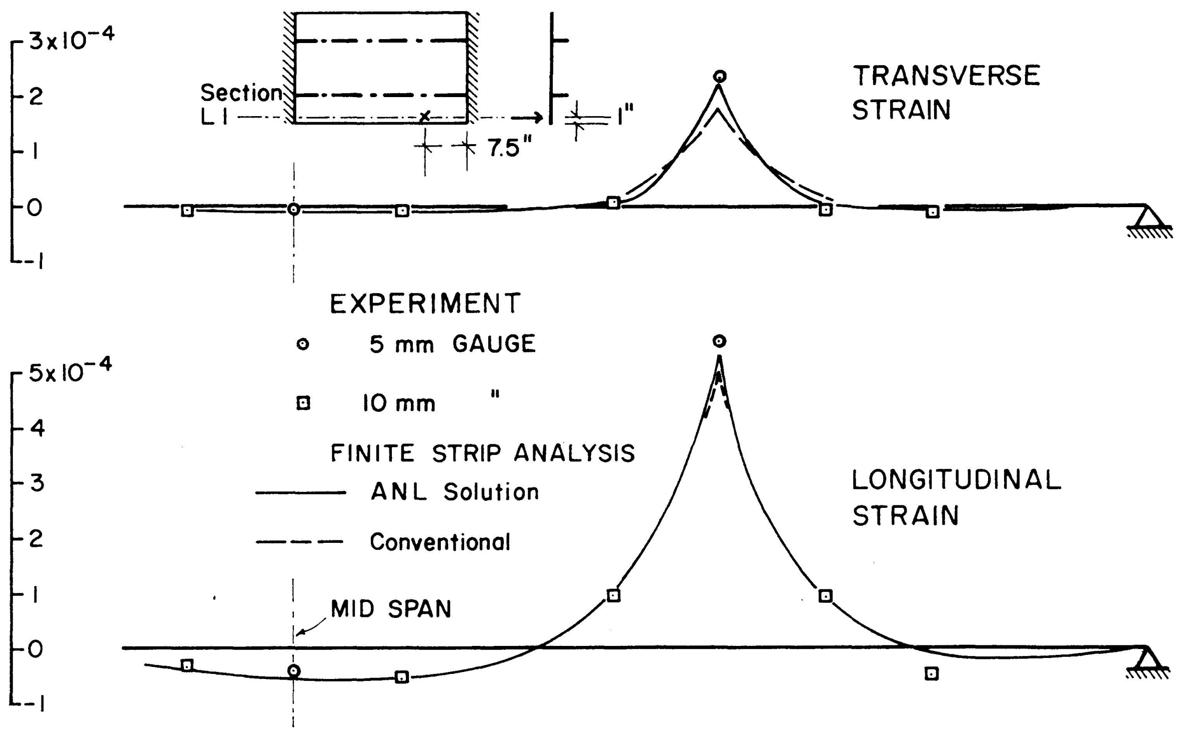

Fig. 14.

bending function incorporated in the conventional program is comparatively less flexible in the transverse direction. The inability of this function to produce a rapidly varying strain field led to this discrepancy. It is interesting to note that for a particular (longitudinal) section the strain profiles due to load applied at different positions along the span are very similar. Evidence may be found

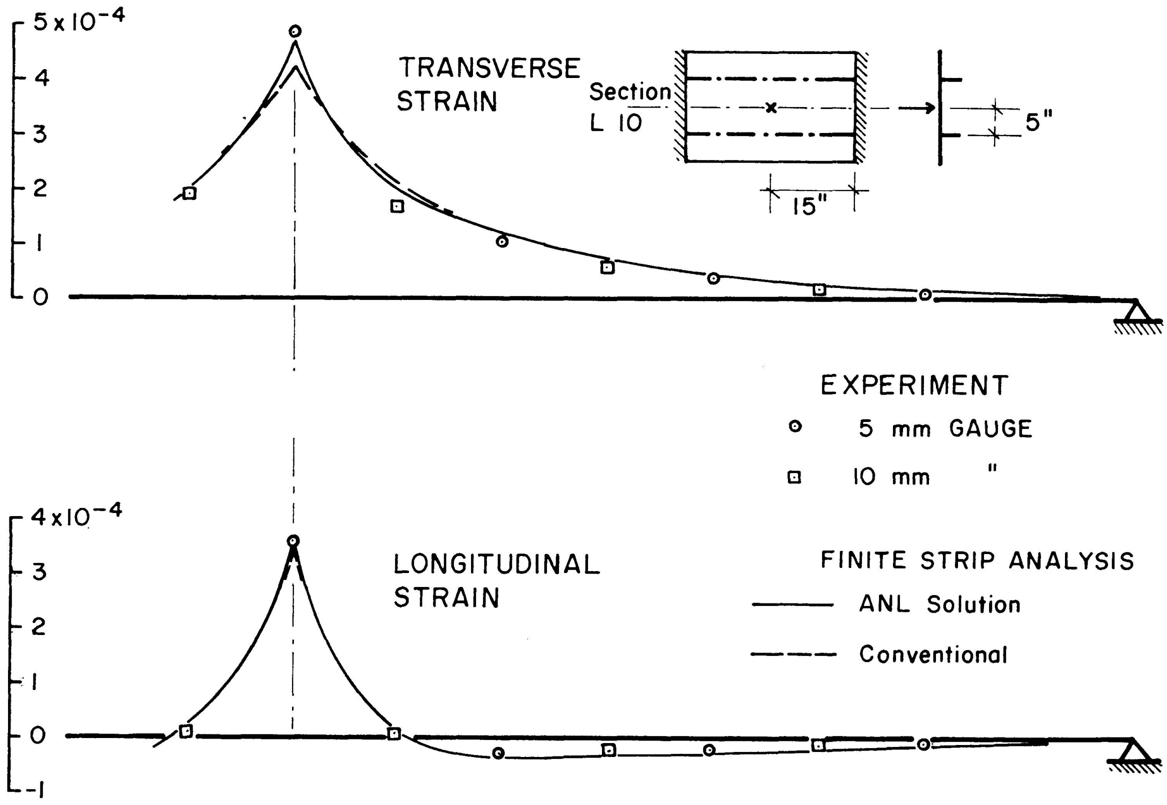
5 x 10^-4
4
3
2
1
0
TRANSVERSE STRAIN
Section L 10
5"
15"
EXPERIMENT
5 mm GAUGE
10 mm "
4 x 10^-4
3
2
1
0
-1
LONGITUDINAL STRAIN
FINITE STRIP ANALYSIS
ANL Solution
Conventional

Fig. 15.

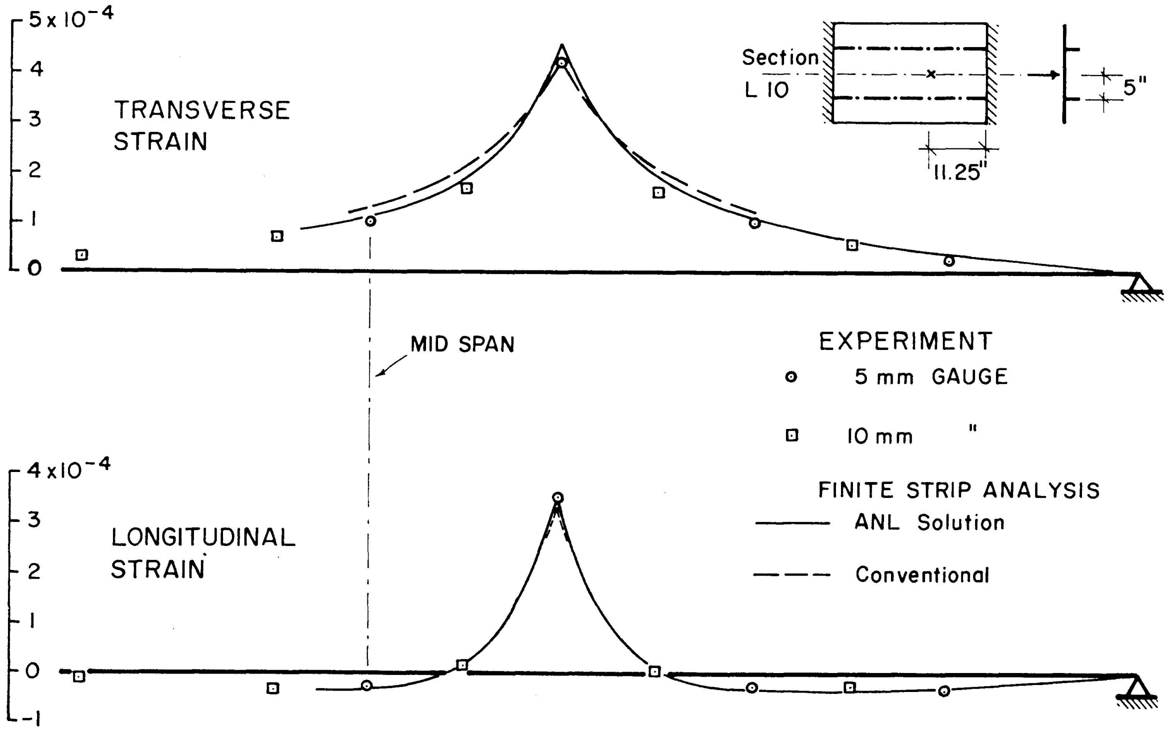
5 x 10^-4
4
3
2
1
0
TRANSVERSE STRAIN
Section L 10
5"
11.25"
MID SPAN
EXPERIMENT
5 mm GAUGE
10 mm "
4 x 10^-4
3
2
1
0
-1
LONGITUDINAL STRAIN
FINITE STRIP ANALYSIS
ANL Solution
Conventional

Fig. 16.

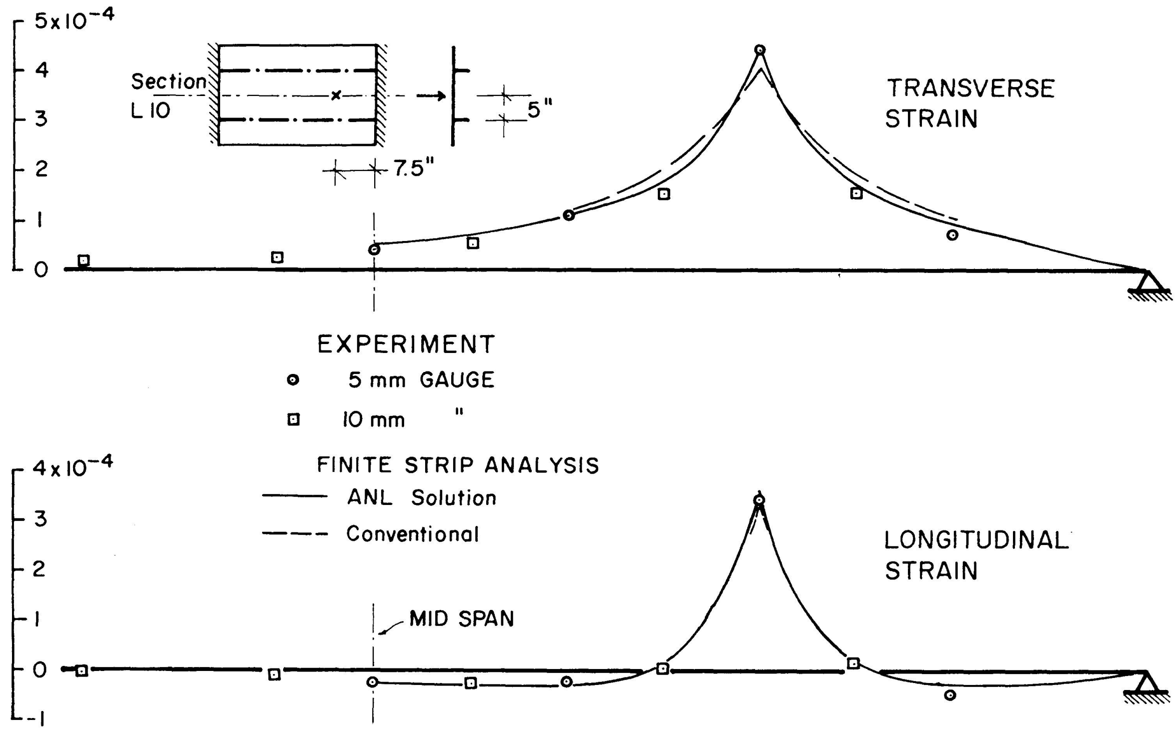
5x10⁻⁴
4
3
2
1
0
Section
L 10
5"
7.5"
TRANSVERSE
STRAIN
EXPERIMENT
5 mm GAUGE
10 mm "
4x10⁻⁴
3
2
1
0
-1
FINITE STRIP ANALYSIS
ANL Solution
Conventional
LONGITUDINAL
STRAIN
MID SPAN

Fig. 17.

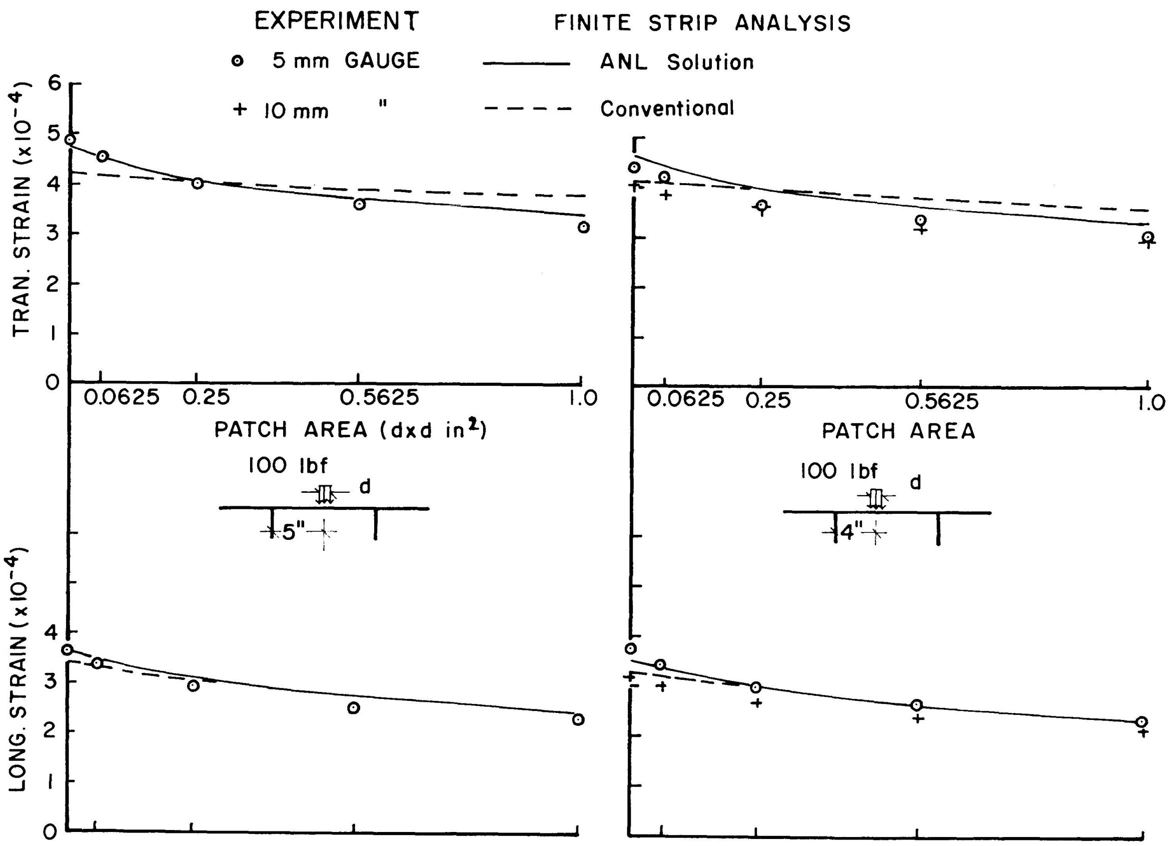
EXPERIMENT
5 mm GAUGE
+ 10 mm "
FINITE STRIP ANALYSIS
ANL Solution
Conventional
TRAN. STRAIN (x10⁻⁴)
6
5
4
3
2
1
0
0.0625 0.25 0.5625 1.0
PATCH AREA (dxd in²)
100 lbf
d
5"
0.0625 0.25 0.5625 1.0
PATCH AREA
100 lbf
d
4"
LONG. STRAIN (x10⁻⁴)
4
3
2
1
0

Fig. 18.

by comparing Fig. 13 with Fig. 14 or Fig. 15 with 16 and 17. Although no comparison is presented in the previous section, similar phenomenon has been found for the transverse distribution of strains. This again implies that the design for local bending moments can be based on analysis of one transverse section only.

Effect of Patch-Load Area on the Distribution of Strains

In order to study the change in strain distribution curves due to a different load intensities over different areas, patch loads were applied at the three central load positions at mid-span of the model. The experimental strain values for different patch intensities are plotted for the two load positions in Fig. 18 together with the theoretical curves by the two finite strip programs. It is shown in Fig. 18 that the ANL program gives results of transverse and longitudinal strains close to the experiments. The lower order analysis, however, underestimates the transverse strains for small patch load while over-

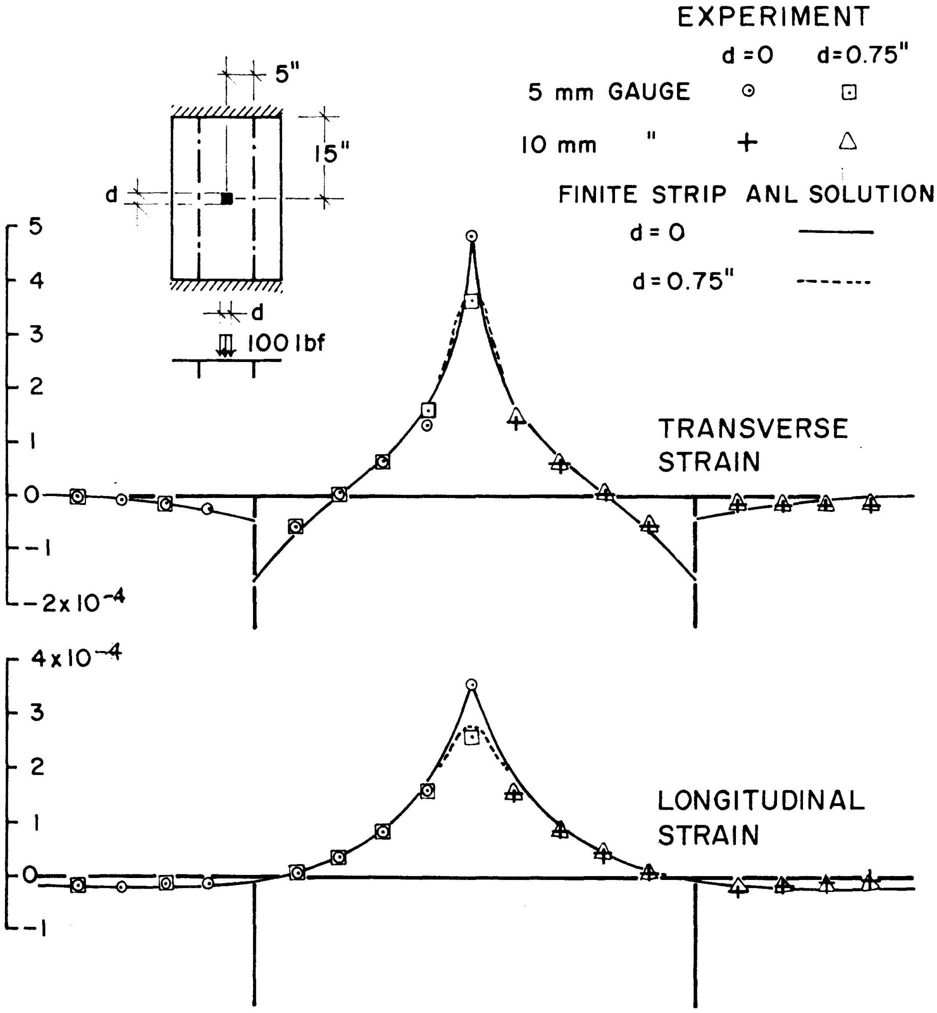

Fig. 19.

estimating the same values for large patches. Since a third order displacement function is incorporated in the conventional program, it thus results in yielding a mainly straight-line variation for transverse moments across the width of a strip. The inability of this linearized variation of transverse moment to conform to the convex moment induced by large patch areas is thought to be mainly responsible for the overestimate by the conventional procedure.

In Fig. 19 the transverse distribution of strains due to a concentrated load of 100 lbf is compared with that induced by the same load but distributed over an area of 0.5625 in^2 (0.75×0.75). It can be seen that apart from those in the vicinity of the load, the strains are practically identical for the two loading conditions.

Distribution of In-Plane Strains at Beams

The influence lines of longitudinal in-plane strains for three positions at the bottom fibres of the left-hand beam are given in Fig. 20. It is obvious from the figure that the strain distributions are overestimated by the two finite strip programs. It was at first thought that the heavy end diaphragms and possible

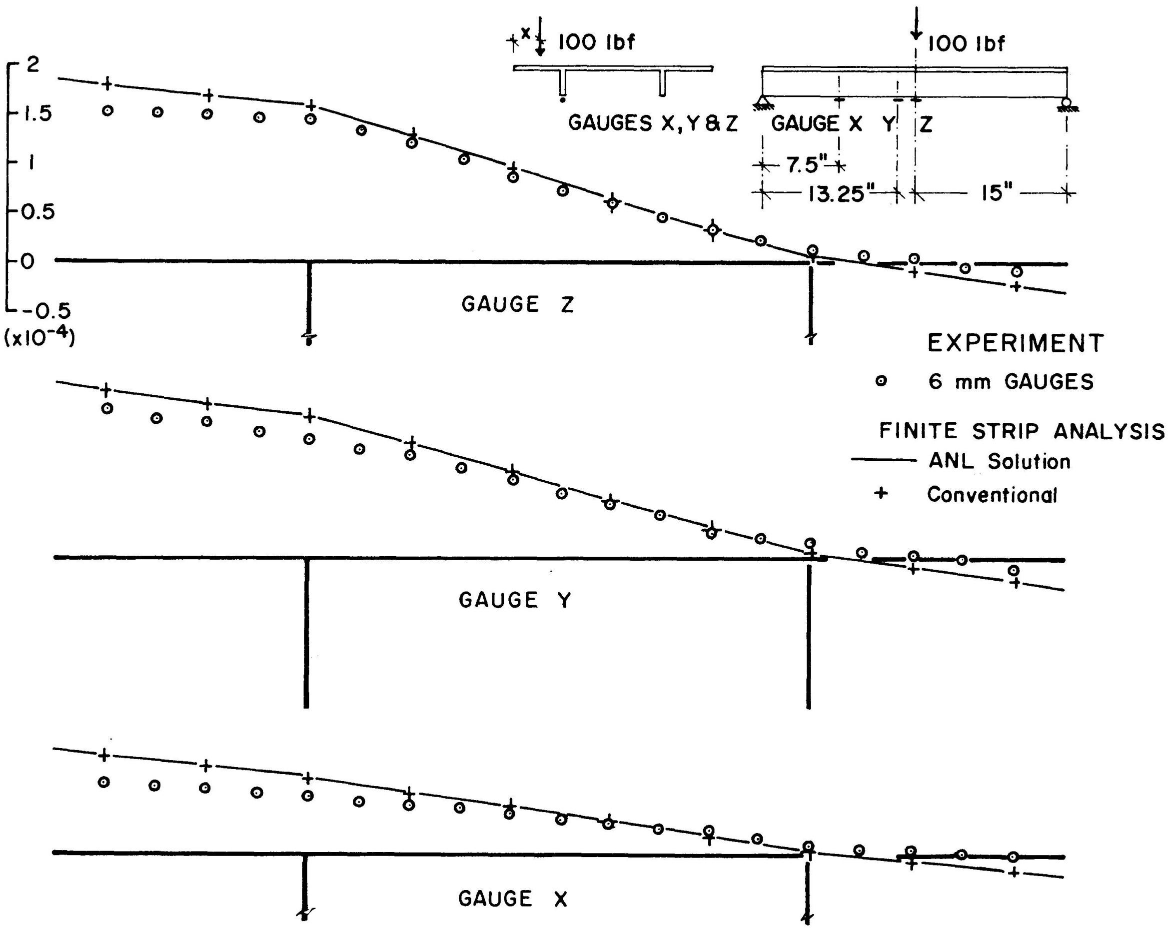

Fig. 20.

partial restraints created by the downward loads applied to the two rollers at the supports (see Fig. 2) were responsible for this considerable discrepancy. Later on, the possible friction at the supports induced by the downwards loads was carefully removed but no significant change was observed. However, before any further conclusion can be made for the accuracy of the method in analysing longitudinal stress more extensive experimental investigation must be carried out.

Comparisons of the Finite Strip ANL Solution and the Westergaard Approach

A number of simple equations have been given by WESTERGAARD [1] for the distribution of moments under concentrated load applied on a simply-supported infinite strip. Thin plate theory was used to derive the equations for moment at any point outside the vicinity of the applied load. For maximum bending moments immediately under the applied load, "equivalent" formulae have been obtained with the help of a special plate theory due to A. Nadai. The complete distribution of moments may therefore be achieved by an interpolation using the thin plate equations and the equivalent formulae.

To investigate the accuracy of the Westergaard equations, comparisons are made with the ANL program on the T-beam model. Fig. 21a shows the maxi-

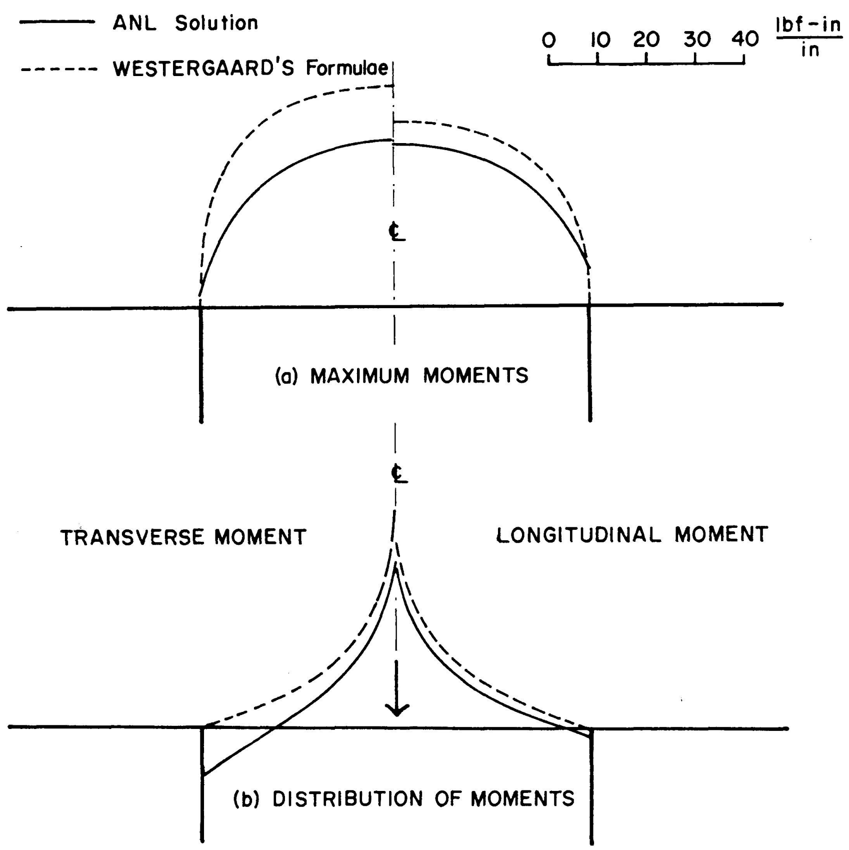

Fig. 21.

mum bending moments under a concentrated load of 100 lbf moving across the width of the slab between beams. It should be noted that the Westergaard analysis does not cover the case when load is applied at the cantilever slab. The transverse distribution of bending moments for a concentrated load acting at the centre of the bridge is plotted in Fig. 21b. It may be seen in Figs. 21a and 21b that the Westergaard solution tends to overestimate the results especially for the transverse moment. This is probably attributable to the simple support assumptions adopted in the Westergaard analysis. However, in view of the simplicity and wide availability of the formulae, the analysis remains a useful tool for preliminary design.

Conclusions

The distribution of local strains in an approximately $^1/_{30}$ scale beam and slab bridge model has been investigated. Electrical resistance strain gauges with 5 mm gauge length were found to be comparatively more effective than the 10 mm gauges in measuring peak strains. A good correlation of the distribution of strains was found between the finite strip analyses and the experimental results.

Experimental and theoretical investigations reveal that the support conditions will not effectively alter the local plate bending moment profiles for a box-type bridge deck under concentrated loads. Thus, for a bridge of this type, it is justifiable to base the design for local plate bending moments under vehicle loading on the analysis of any appropriate transverse section of the deck.

Comparisons with experimental results show that the finite strip solution based on the strip with one auxiliary nodal line is superior to the conventional procedure in predicting local plate bending moments in the beam and slab model. The superiority lies in the fact that the rate of convergence is higher for the ANL solution using the same discretization pattern. Such improvement of accuracy can be expected in the analysis of other folded-plate type bridge decks.

Acknowledgements

The work described in this paper forms part of the research project on concrete multicellular bridge decks sponsored by the British Construction Industry Research and Information Association at the Civil Engineering Department, Dundee University. The author is grateful to the Association for permission to publish these results in this form. The author is also indebted to Professor A. R. Cusens, the project supervisor, for his constructive suggestions and encouragement throughout the course of this work. The experiments were performed at the Structural Engineering Laboratory and the computing work was carried out in the University Computing Centre. The assistance received from the technical staff of these two laboratories is gratefully acknowledged.

References

1. H. M. WESTERGAARD: Computation of stresses in bridge slabs due to wheel loads. Public Roads. Vol. 11, No. 1, March 1930, p. 1.
2. F. SAWKO, and J. H. MILLS: Design of cantilever slabs for spine beam bridges. Developments in Bridge Design and Construction (Edited by K. C. Rockey et al.). Crosby Lockwood Ltd., London, 1971, p. 1.
3. A. R. CUSENS, and R. P. PAMA: Distribution of concentrated loads on orthotropic bridge decks. The Structural Engineer, Vol. 47, No. 9, September 1969, p. 377.
4. P. T. K. LIM, and K. R. MOFFATT: Finite element analysis of curved slab bridges with special reference to local stresses. Developments in Bridge Design and Construction. Crosby Lockwood Ltd., London, 1971, p. 27.
5. Y.-K. CHEUNG: Analysis of box girder bridges by finite strip method. Proc. Second Intl. Symposium on Concrete Bridge Design, Chicago, April 1969, ACI Publn. SP 26, p. 357.
6. A. C. SCORDELIS: Analytical solutions for box girder bridges. Developments in Bridge Design and Construction. Crosby Lockwood Ltd., London, 1971, p. 200.
7. Y.-C. LOO, and A. R. CUSENS: Developments of the finite strip method in the analysis of bridge decks. Developments in Bridge Design and Construction. Crosby Lockwood Ltd., London, 1971, p. 53.
8. Y.-K. CHEUNG: Folded plate structures by finite strip method. Proc. ASCE Vol. 95, No. ST 12, December 1969, p. 2963.
9. Y.-C. LOO, and A. R. CUSENS: The auxiliary nodal line technique for the analysis of box girder bridge decks by the finite strip method. Paper presented at the McGill-EIC Conference on Finite Element Method in Civil Engineering, McGill University, Montreal, Canada, June 1972. Conference Proceedings, p. 995.

Summary

The paper summarises the experimental details and results for strain of a $^1/_{30}$ scale asbestos cement T-beams bridge model tested under concentrated load. The results are plotted against two finite strip analyses developed for folded plate type bridge decks. In the light of the experimental data, the comparative accuracy of the two analyses in predicting local plate bending moments under concentrated loads is discussed.

Résumé

Le travail résume les détails expérimentaux et les résultats de la sollicitation d'une poutre T en amiante-ciment sur un modèle de pont à l'échelle de

1 à 30 mis à l'essai sous charge concentrée. Les résultats sont mis en opposition aux deux analyses de bande finies qui ont été développées pour des tabliers en plaques pliées. Sous l'aspect des dates expérimentales l'exactitude comparative des deux analyses, en prédisant les moments de flexion locaux des plaques sous l'effet d'une charge concentrée est discutée.

Zusammenfassung

Die Arbeit fasst die experimentellen Einzelheiten und Versuchs-Ergebnisse der Beanspruchung eines Asbest-Zement-T-Balkens an einem Brückenmodell im Massstab 1 : 30 unter konzentrierter Last zusammen. Die Ergebnisse werden den zwei endlichen Band-Analysen gegenübergestellt, die für gefaltete Platten-Brückenfahrbahnen entwickelt wurden. Im Lichte der experimentellen Daten wird die vergleichende Genauigkeit der beiden Analysen für örtliche Plattenbiegungsmomente unter konzentrierter Last voraussagend diskutiert.

Leere Seite
Blank page
Page vide